LRP 448/92 January 1992

APPLICATION OF A NEW ALGORITHM TO PLASMA SHAPE CONTROL IN BPX

F. Hofmann, N. Pomphrey and S.C. Jardin

submitted for publication in Nuclear Fusion

APPLICATION OF A NEW ALGORITHM TO PLASMA SHAPE CONTROL IN BPX

F. Hofmann*, N. Pomphrey, S.C. Jardin

Plasma Physics Laboratory, Princeton University
P.O. Box 451, Princeton, New Jersey 08543, USA

submitted for publication in Nuclear Fusion

* permanent address:
Centre de Recherches en Physique des Plasmas,
Association Euratom - Confédération Suisse,
Ecole Polytechnique Fédérale de Lausanne,
21 Avenue des Bains, CH-1007 Lausanne, Switzerland.

APPLICATION OF A NEW ALGORITHM TO PLASMA SHAPE CONTROL IN BPX

F. Hofmann*, N. Pomphrey, S.C. Jardin

Plasma Physics Laboratory, Princeton University
P.O. Box 451, Princeton, New Jersey 08543, USA

Abstract

A new shape control algorithm has been tested by numerical simulation of a tokamak discharge in the Burning Plasma Experiment (BPX), using the TSC code. The algorithm controls the plasma shape and current according to a preprogrammed scenario without using any precalculated coil current waveforms. If the plasma parameters (heating scenario, density evolution, Z_{eff}, etc.) change, the algorithm automatically maintains the given shape evolution and does not have to be readjusted. This allows independent programming of plasma current, density, heating power, shape and position.

* permanent address:
Centre de Recherches en Physique des Plasmas,
Association Euratom - Confédération Suisse,
Ecole Polytechnique Fédérale de Lausanne,
21 Avenue des Bains, CH-1007 Lausanne, Switzerland.

1. Introduction

The classical method of controlling the plasma shape and position in an elongated tokamak [1-3] is based on the assumption that the current in each of the poloidal field coils is the sum of a preprogrammed current and a correction current, the latter being a small fraction of the former. Preprogrammed current waveforms can be obtained from a sequence of MHD equilibria, simulating the desired plasma evolution. The correction currents, on the other hand, are computed in real time so as to adjust the plasma position and shape.

The classical approach has one major shortcoming: If the plasma parameters in a real discharge turn out to be very different from the ones which were assumed in computing the preprogrammed currents, the correction currents may become large and the shape accuracy suffers. Under these circumstances, one is forced to adopt a learning strategy with the aim of improving the performance shot after shot.

These problems can be overcome by using an advanced algorithm which computes the poloidal field coil currents directly, in real time, without requiring any precalculated current waveforms as input. Such algorithms involve a volume of real-time computing which is considerably larger than what is necessary with classical algorithms. Fortunately, however, the advent of fast digital array processors and hybrid computers has made the implementation of advanced algorithms entirely feasible [4].

In this paper, we test an advanced shape control algorithm [4] of the type described above by simulating a complete discharge in the Burning Plasma Experiment (BPX) [5]. The simulation is performed by means of the Tokamak Simulation Code (TSC) [6].

2. Algorithm

The control algorithm has been described in detail in Ref.[4]. Here, we only give a brief summary of the main concepts. The basic idea is to control the poloidal flux at a number of points at the plasma boundary. The coordinates of these points are preprogrammed functions of time. They define the desired shape evolution. The control algorithm computes flux errors at the preprogrammed boundary points, in real time, by reconstructing the plasma current distribution in the form of a finite element matrix. It then computes coil current increments and coil voltages.

The algorithm consists of four basic elements (Fig.1.): The first is a matrix, A, which converts the vector of measurements (coil currents, flux loops, magnetic field probes, etc.) into a vector of error signals (flux errors, magnetic field errors, positional error, plasma current error, etc.). This matrix depends on a number of preprogrammed functions (coordinates of boundary points, desired plasma current, etc.). It involves the reconstruction of the plasma current in the form of a set of finite elements [7] and it computes flux and magnetic field errors at the preprogrammed boundary points.

The second element consists of a number of PID controllers which act on the error signals and whose gain coefficients are adjusted for optimum closed-loop stability.

The third element is again a matrix, M^{-1}, which calculates the rate of change of the poloidal field coil currents, such as to obtain the maximum possible error reduction. This is achieved by minimizing a cost functional of the form

$$C = \sum_i \alpha_i \varepsilon_i^2 + d \sum_j \beta_j I_j^2 \qquad (1)$$

where ε_i are the error signals, I_j are coil currents, and α_i β_j are weighting coefficients. The α_i 's are usually assumed to be unity, whereas the β_j 's are chosen such that the second term on the r.h.s. of Eq. (1) becomes proportional to the total power dissipation in the poloidal field coils. The parameter, d, controls the trade-off between shape accuracy and power dissipation [4].

The fourth element (matrix L) finally computes the coil voltages which are necessary to produce the desired rate of change of the coil currents.

The matrices A and M^{-1} will in general vary with time, since they depend on the preprogrammed functions. However, they do not depend on the plasma parameters (β_p, l_i, q_o, etc.) and no MHD equilibrium calculations are required to generate these matrices.

The response time of this system is limited by the performance of the on-line control computer and by the finite bandwidth of the power electronics. It has been shown [4] that response times of the order of 1 ms can easily be obtained using conventional technology. For the present application, i.e. shape control of a large tokamak, response times as large as 10 ms would still be adequate.

3. TSC Simulation

3.1. BPX Reference Scenario

As an application of the control algorithm let us consider a numerical simulation of the proposed Burning Plasma Experiment (BPX), in which the plasma current and toroidal magnetic field are preprogrammed as shown in Fig.2. The current is ramped linearly in time from the initial value I_p= 100 kA at time t=0.0 sec to the flattop value of I_p= 11.8 MA at t=7.5 sec. During this interval, the toroidal field is increased from B_t =7.4 T to B_t =9.0 T. The current and toroidal field flattop period extends until t=13.2 sec. The plasma current rampdown is piecewise linear in two stages: First the current is decreased at 1.6 MA/sec for 4.5 sec. Then it is decreased at a rate of 0.8 MA/sec to a final value of 100 kA at t=23.7 sec. During the plasma current rampdown the toroidal field is decreased exponentially in time, with a time constant of 11.0 sec.

Fig 3. shows a plot of the plasma power balance as a function of time. To assist heating of the plasma, 10 MW of ICRH heating is supplied at t=4.5 sec, and this is increased to 20 MW beginning at t=5.5 sec. When the total heating power, $P_{heat} = P_{\alpha} + P_{ohmic} + P_{ICRH}$ reaches 100 MW the TSC code instantaneously adjusts the value of P_{ICRH} in order to maintain P_{heat} = 100 MW. The auxiliary heating is turned off at the end of flattop.

The shape evolution during the simulation is shown in Figs. 4,5 and 6. The plasma is grown from an outboard limited circular plasma at t=0.0 sec, becomes double-null diverted at t=4.0 sec, and achieves a maximum elongation of κ_{95}=2.1 at the beginning of the current flattop phase. During the current flattop, the plasma elongation is decreased to κ_{95}=2.0 while the plasma triangularity is increased from δ_{95}=0.25 to 0.44 in order to effect a 0.20 m sweep of the outboard separatrix strike point across the divertor plate surface. Minimum separation distances from the plasma X-point to the divertor plate are required to be 0.15 m for the outboard strike point and 0.10 m for the inboard strike point. Upon completion of the divertor sweep, the plasma major radius is immediately decreased to force the plasma to be limited on the inboard edge and thereby decrease the heat load in the divertor region. The final plasma, at the end of the rampdown phase is inboard limited and circular in shape. Full details of the modelling of this BPX discharge scenario can be found in Ref. [5].

3.2. Measurements

The shape control algorithm outlined in section 2 requires measurements of coil currents, vacuum vessel currents, plasma current, poloidal fluxes and poloidal magnetic fields as input quantities. Here, we assume that the flux loops and magnetic field probes are located on the vacuum vessel wall, as shown in Fig. 4. Thirty-four flux loops and thirty-four magnetic field probes are distributed uniformly over the wall contour. The magnetic probes are assumed to be oriented parallel to the wall. Vacuum vessel currents are neglected in this study. This is justified by the fact that the L/R time for the penetration of a vertical field into the BPX vessel is 38.1 ms, whereas characteristic times for shape control are much longer.

Flux and magnetic field measurements are simulated in the TSC code by interpolation of the Ψ values at the discrete mesh point locations. Errors due to the finite mesh size are typically of the order of 1%. We do not add any additional errors to these measurements. The effect of random errors on the precision of the shape evaluation has been investigated elsewhere [7].

3.3. Preprogrammed Plasma Shape

For the simulation described in this paper, we define the desired plasma shape at a number of time values (t=0, t=2.25, t=3.5, t=4.25, t=7.5, t=13.2, t=15.0, t=21.7 and t=23.7 sec) by assigning values to the R and Z coordinates of twenty boundary points which lie on the desired plasma-vacuum interface. Between any two time values, e.g. t_1 and t_2, the coordinates of the boundary points change according to the interpolation scheme

$$R_n(t) = R_{n,1} + g(t)\,\{R_{n,2} - R_{n,1}\} \qquad , n=1...20$$

$$Z_n(t) = Z_{n,1} + g(t)\,\{Z_{n,2} - Z_{n,1}\} \qquad , n=1...20 \qquad (2)$$

where $R_{n,1}$, $Z_{n,1}$ and $R_{n,2}$, $Z_{n,2}$ are the coordinates of the n-th boundary point at times $t=t_1$ and $t=t_2$, respectively. Here, the interpolating function g(t) is assumed to have the simple form

$$g(t) = 1 - ((t_2-t)/(t_2-t_1))^h \qquad (3)$$

where h is a constant normally chosen to be 1. The form of g(t) can be chosen to ensure monotonicity of the edge safety factor with respect to time, if desired. The evolution of the boundary points is illustrated in Fig.5. where only the time values t=0.0, t=2.25, t=7.5 and t=13.2 sec are shown.

3.4. Plasma Current Programming

The plasma current is preprogrammed as shown in Fig.2. In the TSC simulation, the plasma current is controlled by a feedback loop, acting on the total Volt-secs linked by the poloidal field coils to a chosen reference point. This is implemented by introducing an additional error term in the cost functional (eq. 1) of the form

$$\varepsilon_{vs}^2 = \gamma(I_p^a - I_p^p)^2 \qquad (4)$$

where ε_{vs} is considered to be an error in the total flux produced by all coils at the reference point (R=2.97m, Z=0), $I_p{}^a$ and $I_p{}^p$ are the actual and preprogrammed values of the plasma current, respectively, and γ is a feedback gain.

3.5. Finite Element Geometry

In order to compute accurate flux values at the preprogrammed boundary points, we reconstruct the plasma current distribution in the form of a finite element matrix [7]. The number of elements is chosen such that there are always two elements in the radial direction and

that the base of each element is roughly square. In principle, the number and geometry of the elements can remain fixed during the entire shape evolution [4]. In BPX however, this scheme would not give accurate results because the initial plasma cross section is very small compared to the cross section at full plasma current. If the finite elements were fixed, the initial plasma would be represented by only one or two elements, which is insufficient. Consequently, we do not use fixed elements, but we adapt the number and geometry of the elements to the instantaneous, preprogrammed plasma shape, i.e. the width and height of the rectangle defining the outer boundary of the set of elements are periodically adjusted to the width and height of the preprogrammed plasma cross section. This readjustment does not have to be done very frequently. Even if the elements cover an area which is somewhat larger than the plasma, we can still determine the shape of the outermost flux surface with good accuracy [7].

In our BPX simulation, we assume that the initial, circular plasma is represented by six elements, and the final, double-null divertor plasma by ten elements. Since the number of elements is always even, it must change twice during the current ramp-up phase.

3.6. Results

In this section, we present the results of a TSC calculation covering a complete BPX discharge. Fig.2. shows the preprogrammed and actual plasma currents. The two curves fall virtually on top of each other. Fig.6a shows that the outboard edge of the plasma (R+a) is successfully held constant to within 0.0075 m during the heating phase (4.5 sec to 13.2 sec), in spite of the large increase in the poloidal and toroidal beta (Fig.7.). Fig.6b shows evidence of successful control of the elongation and triangularity. At time t=14.3 sec, the discharge switches from diverted to limited, which causes a sudden decrease in ellipticity and triangularity. This explains the relatively large discrepancy between actual and preprogrammed values after t=14.3 sec (Fig.6b). Fig.8. shows that the minimum BPX requirement of a 0.20 m divertor sweep, while keeping the X-point to inner and outer strike point distances at least 0.10 m and 0.15 m, respectively, is satisfied. Finally, the poloidal field coil currents which produce the shape evolution are shown in Fig.9. We note that these coil currents are derived as output from the control algorithm without the need for

preprogrammed input.

4. Conclusions

The shape control algorithm described in Ref.[4] has been successfully applied to the problem of plasma shape control in BPX. A numerical simulation of a complete BPX discharge shows that the actual shape evolution follows the preprogrammed scenario very precisely, although the algorithm makes no assumptions about the plasma beta, internal inductance or other physical parameters. In fact, if the preprogrammed shape is fixed and the plasma parameters change, the algorithm automatically adapts the coil currents to maintain the given shape.

The main advantage of this control algorithm, as compared to other methods, is that the plasma shape on the one hand and the physical plasma parameters on the other hand can be programmed independently. This should greatly simplify tokamak operation since a change in scenario can be implemented easily, without computing sequences of MHD equilibria and without any guesswork concerning the evolution of the plasma parameters.

Acknowledgements

This work was sponsored by the Office of Fusion Energy, U.S. Department of Energy, under contract DE-AC02-76-CHO-3073. The research was partly supported by EURATOM, the Ecole Polytechnique Fédérale de Lausanne and the Fonds National Suisse de la Recherche Scientifique.

References

[1] Bell, R.E., Fishman, H., Hatcher, R., et al., in Fusion Engineering (Proc. 13th Symp. Knoxville, TN, 1989), Vol.1, IEEE, New York (1990) 467.

[2] Ciscato, D., DeKock, L., Noll, P., in Fusion Technology 1980 (Proc. 11th Symp. Oxford, 1980), Vol 2, Pregamon Press, Oxford (1981) 1033.

[3] Luxon, J., Anderson, P., Batty, F., et al., in Plasma Physics and Controlled Nuclear Fusion Research 1986 (Proc. 11th Int. Conf. Kyoto, 1986), Vol. 1, IAEA, Vienna (1987) 159.

[4] Hofmann, F., Jardin, S.C., Nuclear Fusion 30 (1990) 2013.

[5] Goldston, R.S., Jardin, S.C., Bell, M.G., Johnson, J.L. et al: "BPX Physics Design Description Document", WBS-X-910311-PPL-22, to be published in Fusion Technology.

[6] Jardin, S.C., Pomphrey, N., Delucia, J., J. Comput. Phys. 66 (1986) 481.

[7] Hofmann, F., Tonetti, G., Nuclear Fusion 28 (1988) 519.

Figure Captions

Fig.1. Block diagram of control algorithm

Fig.2. Plasma current, I_p (MA), and toroidal magnetic field, B_t (T), versus time, for the TSC simulation of a BPX discharge.

Fig.3. Separate contributions to the calculated power balance, versus time.

Fig.4. Computational grid for the TSC calculation. The poloidal contour of the vacuum vessel wall is shown, with locations of 34 flux loops and magnetic field probes denoted by (x). The locations of the wire filaments representing the seven external poloidal field coils are shown as (o).

Fig.5. Preprogrammed plasma boundary points (upper half plane only) are shown for the time values t=0.0 (.), t=2.25 sec (o), t=7.5 sec (*) and t=13.2 sec (x).

Fig.6 (a) Outboard (R+a) and inboard (R-a) plasma edges, versus time.

Fig.6 (b) Ellipticity (κ) and triangularity (δ) for the plasma edge and the 95% flux surface, versus time. Preprogrammed values for the plasma edge are also shown (open circles, connected with solid lines).

Fig.7 Poloidal (β_ϑ) and toroidal beta (β_t) as functions of time.

Fig.8. Sweep distance, Δs (m), across the divertor plate during the flattop phase, and X-point to strike point distance, $\Delta X_{N\text{-}P}$ (m), versus time.

Fig.9. Poloidal field coil current waveforms for the TSC simulation.

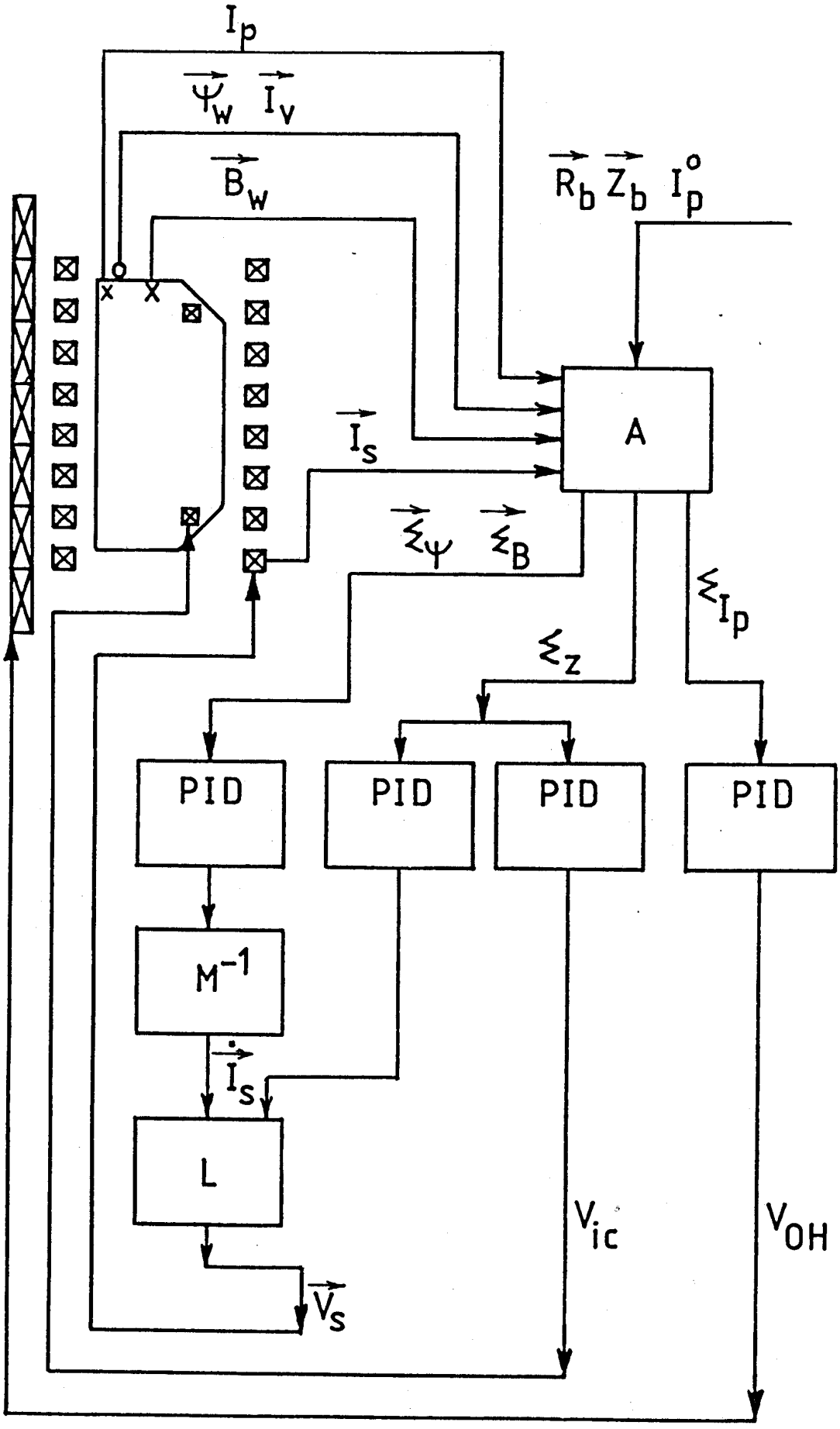
I_p
$\vec{\Psi}_w$ $\vec{I}_v$
$\vec{B}_w$
$\vec{R}_b$ $\vec{Z}_b$ I_p^o
A
$\vec{I}_s$
$\vec{\varepsilon}_\psi$ $\vec{\varepsilon}_B$
ε_{I_p}
ε_z
PID
PID
PID
PID
M^{-1}
$\dot{\vec{I}}_s$
L
V_{ic}
V_{OH}
$\vec{V}_s$

Fig.1.

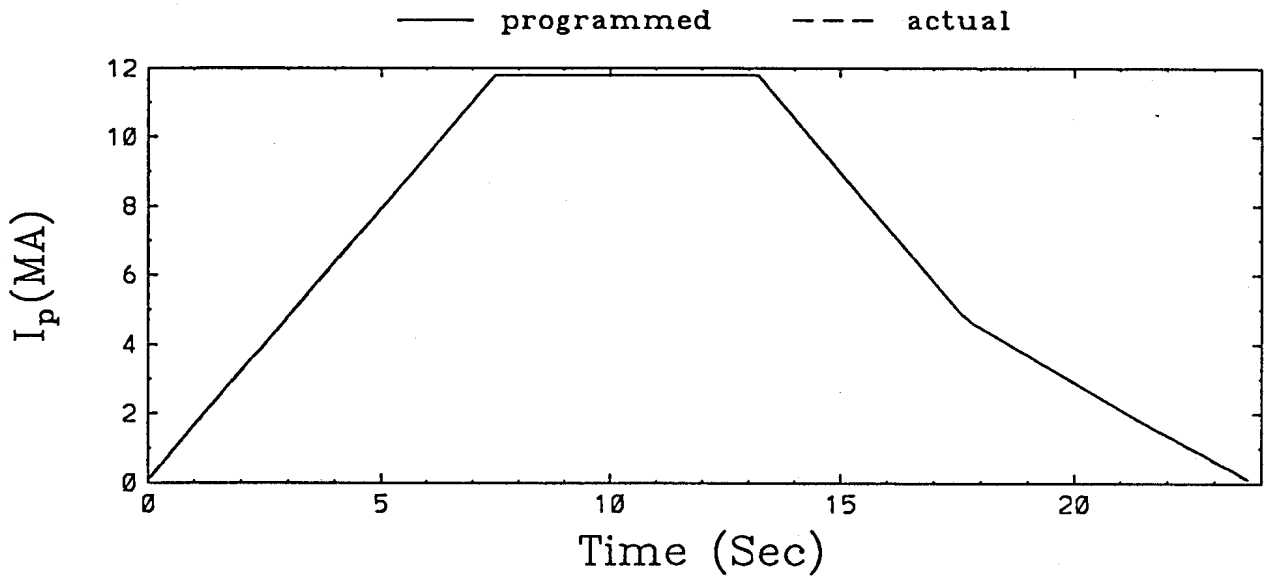
programmed
actual
I_p(MA)
12
10
8
6
4
2
0
0
5
10
15
20
Time (Sec)

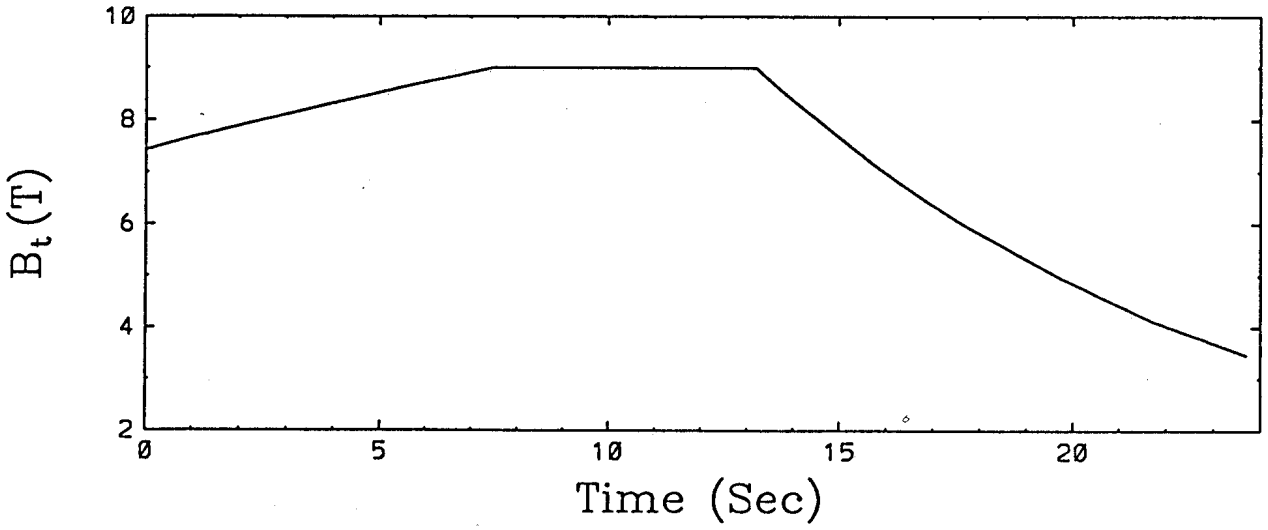
B_t(T)
10
8
6
4
2
0
5
10
15
20
Time (Sec)

Fig.2.

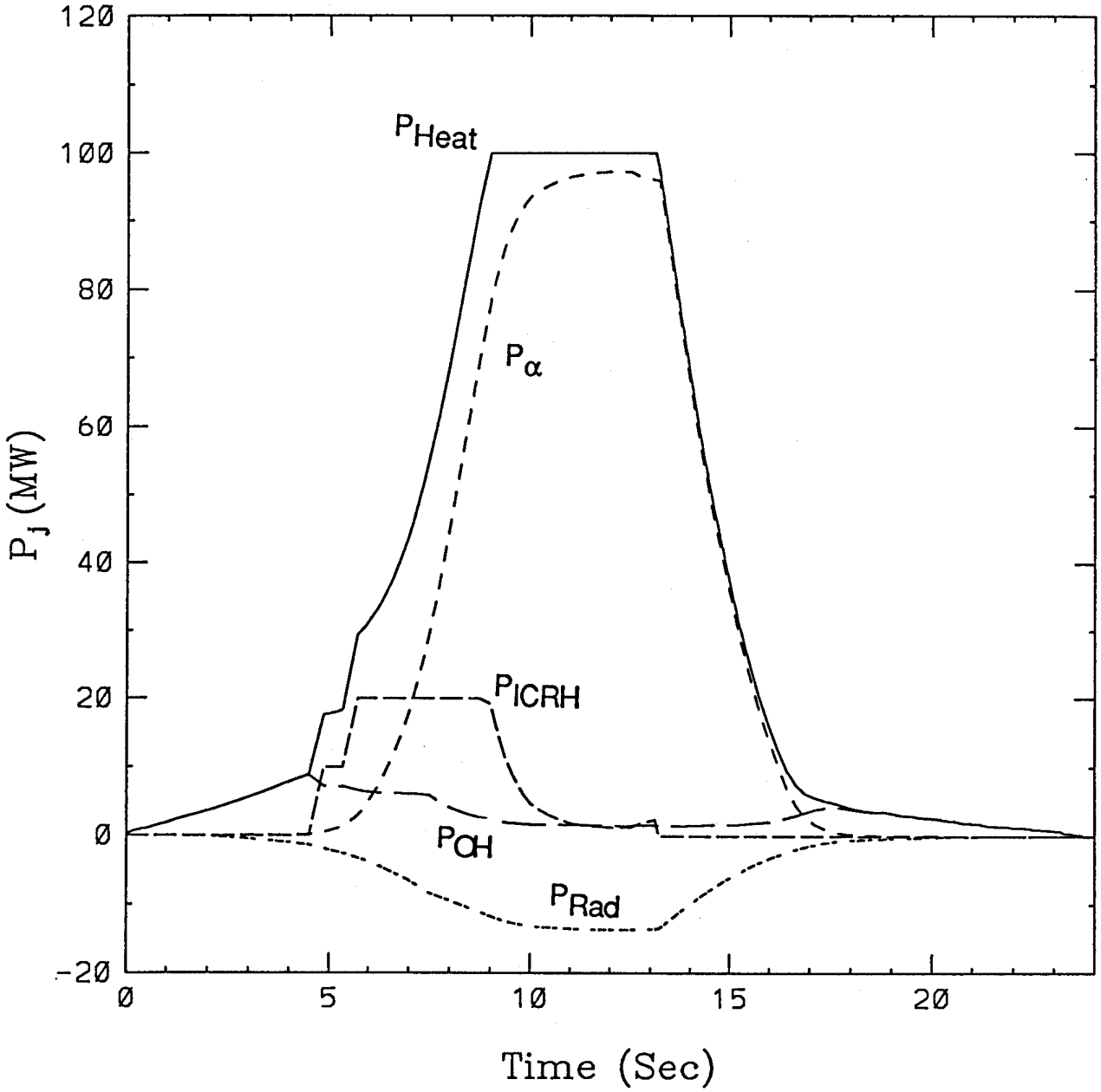
120
100
80
60
40
20
0
-20
0
5
10
15
20
P_j (MW)
Time (Sec)
P_{Heat}
P_α
P_{ICRH}
P_{OH}
P_{Rad}

Fig.3.

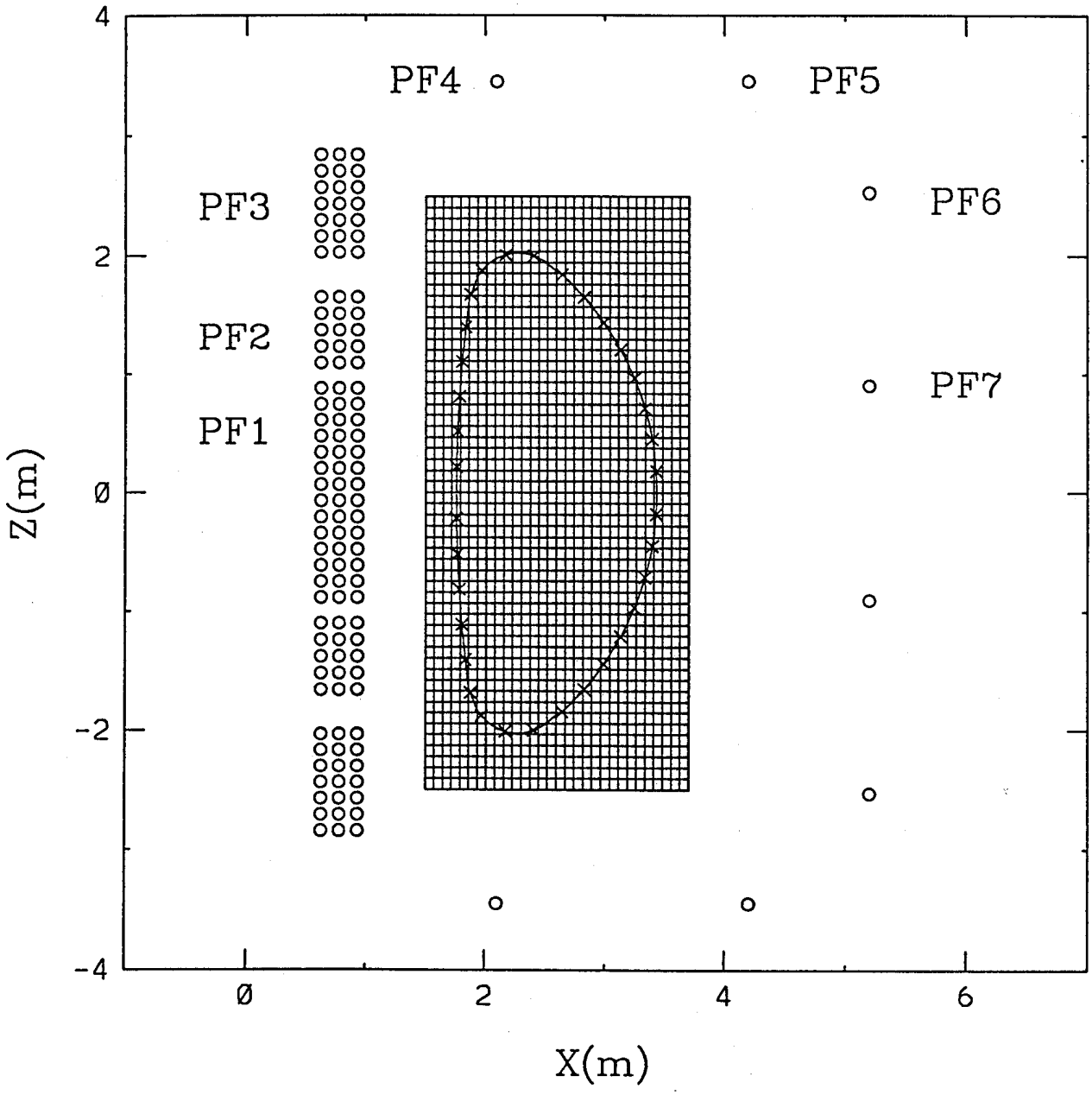

Fig.4.

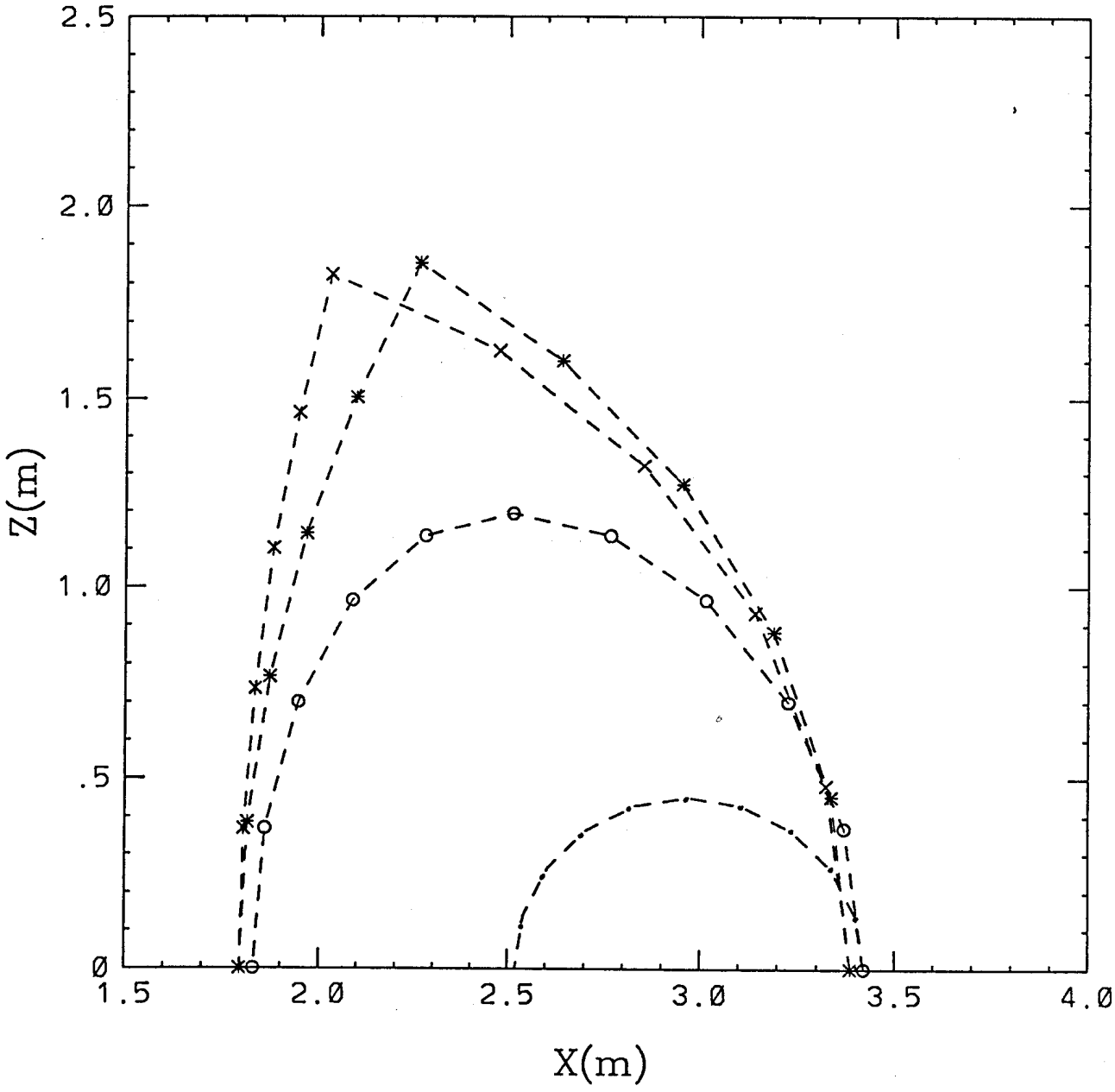

Fig.5.

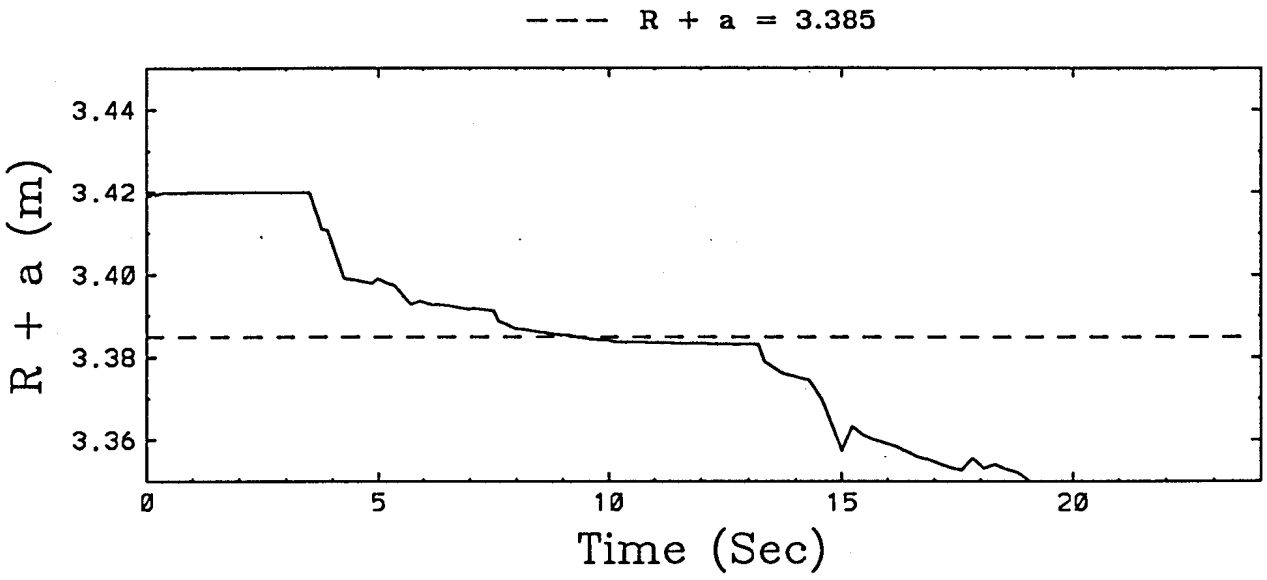
--- R + a = 3.385
3.44
3.42
3.40
3.38
3.36
R + a (m)
0
5
10
15
20
Time (Sec)

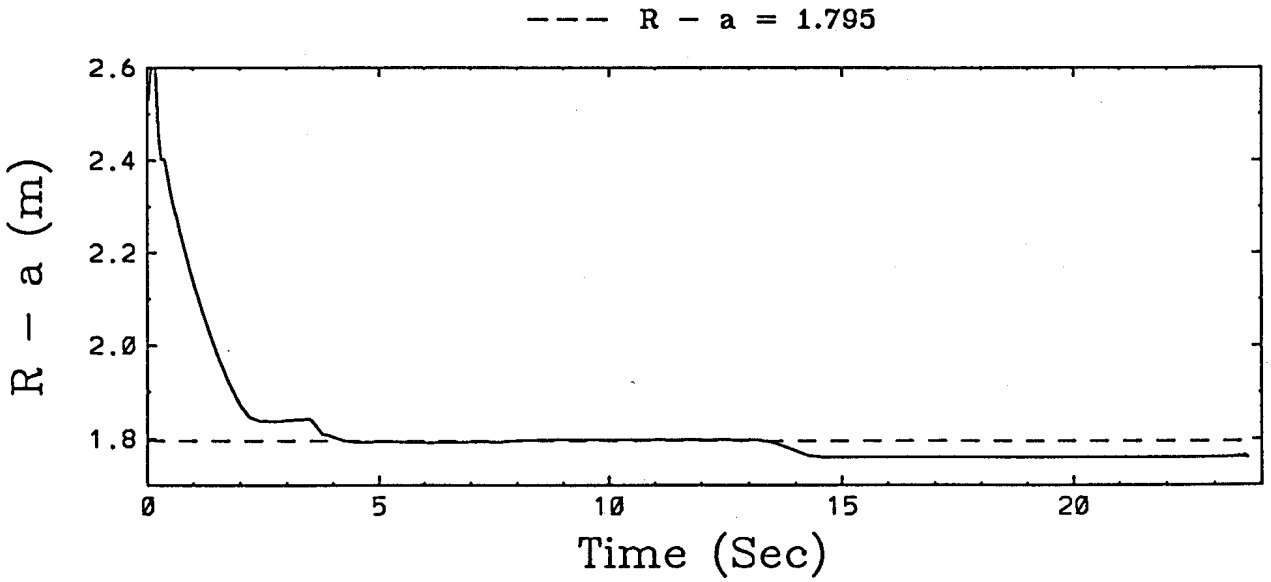
--- R - a = 1.795
2.6
2.4
2.2
2.0
1.8
R - a (m)
0
5
10
15
20
Time (Sec)

Fig.6a.

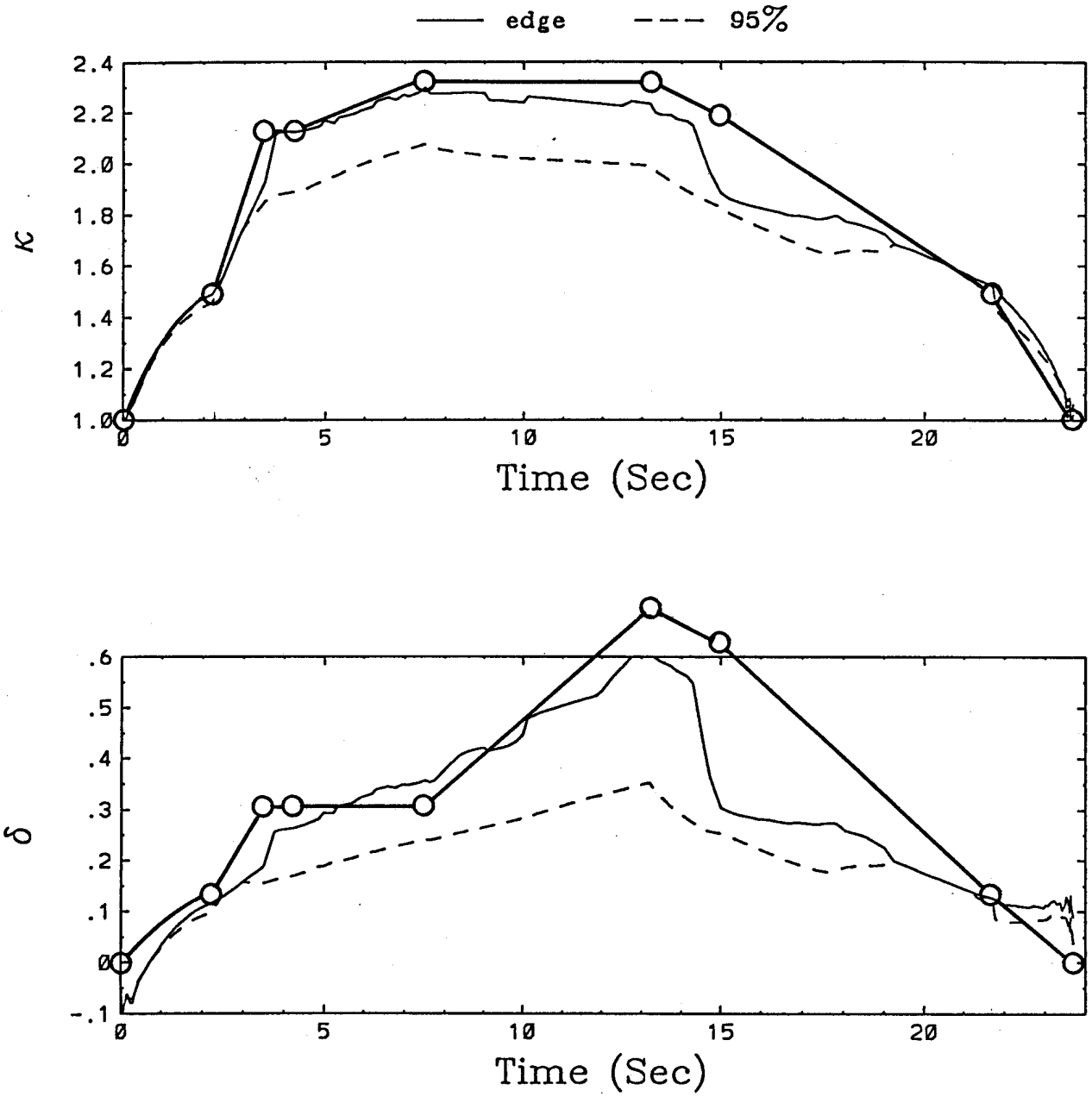
edge
95%
κ
2.4
2.2
2.0
1.8
1.6
1.4
1.2
1.0
0
5
10
15
20
Time (Sec)
δ
.6
.5
.4
.3
.2
.1
0
-.1
0
5
10
15
20
Time (Sec)

Fig.6b.

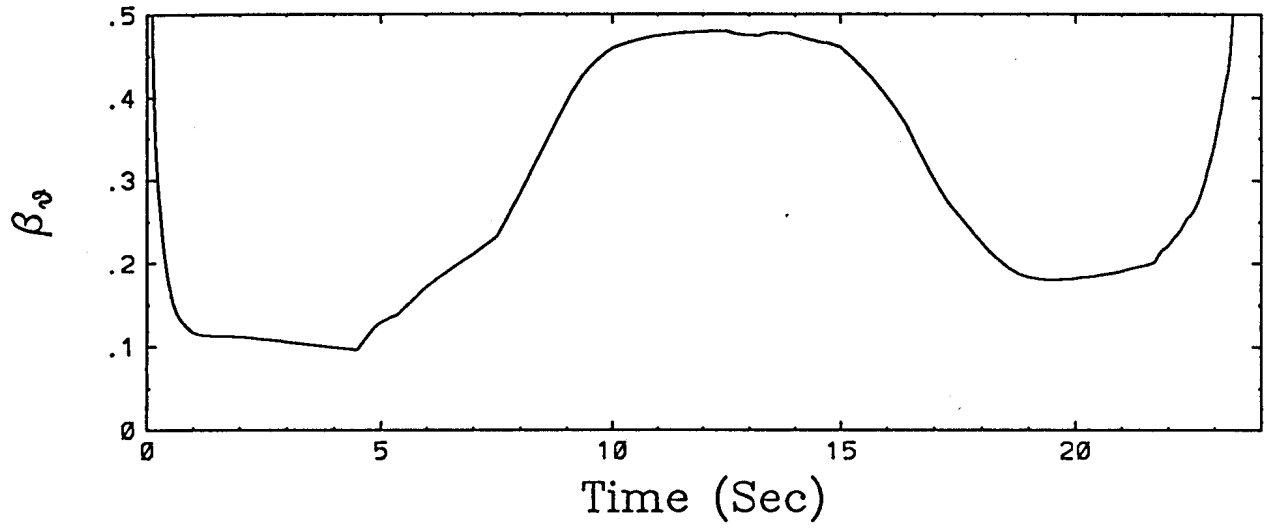
.5
.4
.3
.2
.1
0
β_s
0
5
10
15
20
Time (Sec)

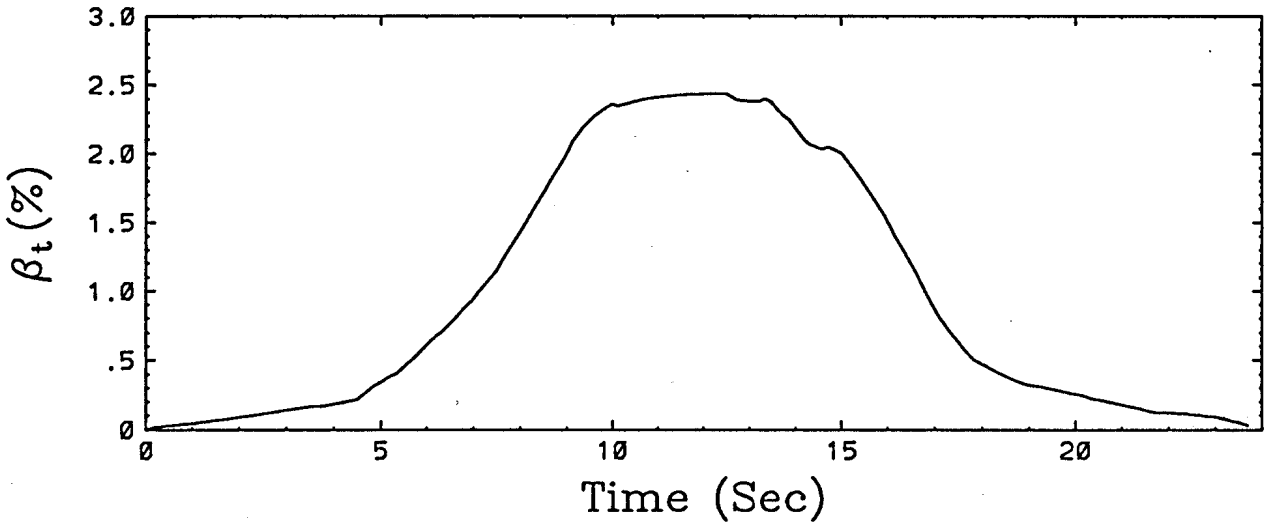
3.0
2.5
2.0
1.5
1.0
.5
0
β_t (%)
0
5
10
15
20
Time (Sec)

Fig.7.

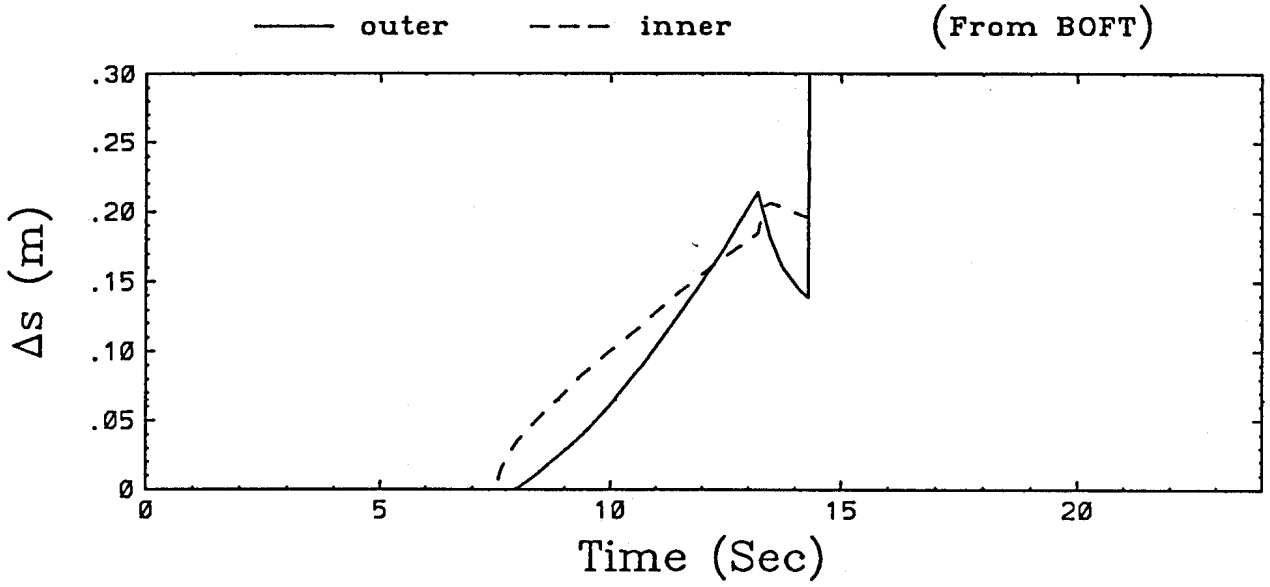
outer
inner
(From BOFT)
.30
.25
.20
.15
.10
.05
0
Δs (m)
0
5
10
15
20
Time (Sec)

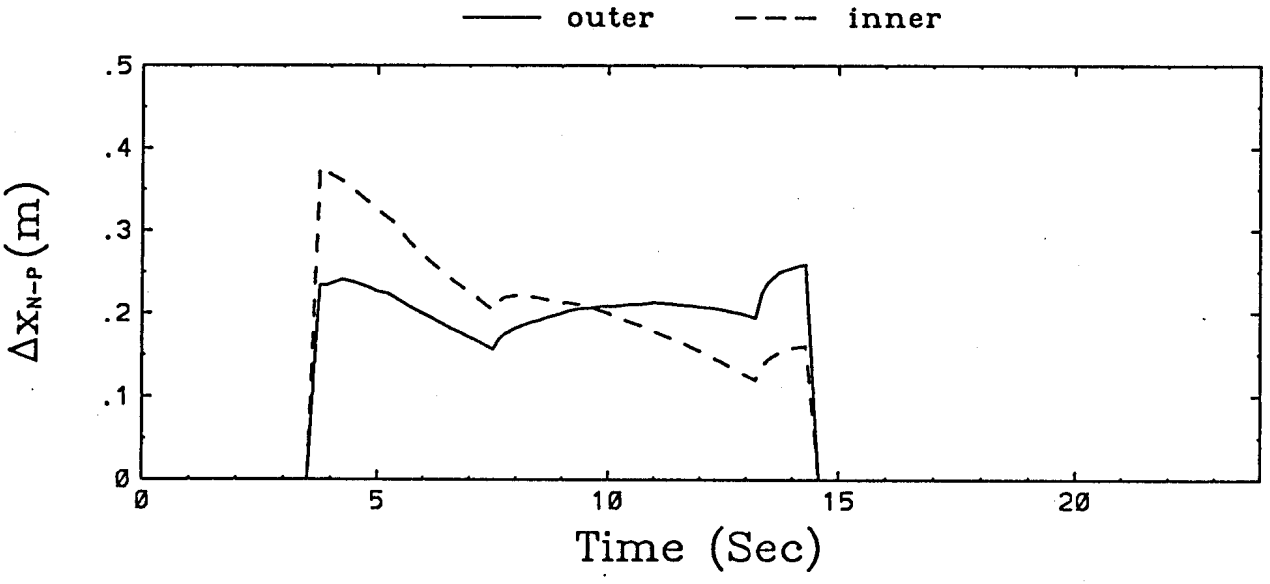
outer
inner
.5
.4
.3
.2
.1
0
ΔXN-P (m)
0
5
10
15
20
Time (Sec)

Fig.8.

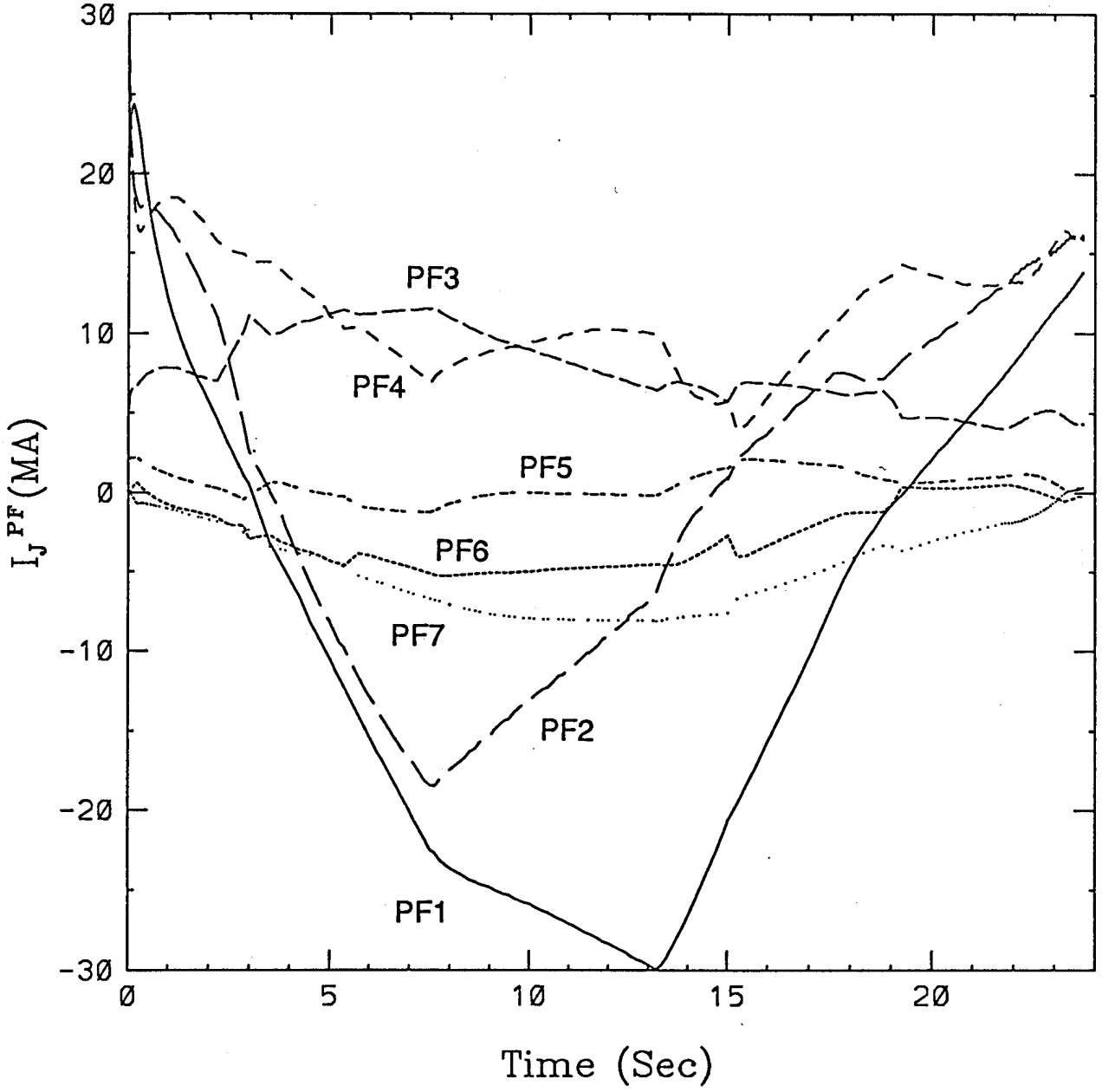
30
20
10
0
-10
-20
-30
0
5
10
15
20
PF3
PF4
PF5
PF6
PF7
PF2
PF1
I_J^{PF} (MA)
Time (Sec)

Fig.9.